

# Interaction Between Dirac Solitons and Jackiw–Rebbi States in Binary Waveguide Arrays

Truong X. Tran, Dũng C. Duong, and Fabio Biancalana

**Abstract**—We systematically study different scenarios of collision between Dirac solitons and Jackiw–Rebbi (JR) states, which have been found recently in a system consisting of two interfaced binary waveguide arrays with opposite propagation mismatches. This collision has the resonance features for the reflected and transmitted signals. The trapping effect of Dirac solitons between two JR-states is analyzed.

**Index Terms**—Binary waveguide arrays, Dirac solitons, Jackiw–Rebbi states, nonlinear fiber optics, nonlinear optical devices, optical switches.

## I. INTRODUCTION

WAVEGUIDE arrays (WAs) have been explored to investigate many fundamental photonic phenomena such as discrete diffraction [1], [2], discrete solitons (DSs) [1], [3]–[5], diffractive resonant radiation [6], and supercontinuum generation in both frequency and wavenumber domains [7], [8]. Waveguide arrays have also attracted a great amount of interest in simulating fundamental effects in nonrelativistic quantum mechanics such as photonic Bloch oscillations [1], [9], [10], and Zener tunneling [11]. On the other hand, binary waveguide arrays (BWAs) - a special class of WAs - present a unique photonic system to investigate relativistic quantum mechanics phenomena arising from the Dirac equation, e.g., *Zitterbewegung* [12], Klein paradox [13], and Dirac solitons in the nonlinear regime [14].

The discrete gap solitons in BWAs in the classical context have been investigated earlier [15]–[18]. But only recently, the discrete solitons in BWAs have been shown to be optical analogs of Dirac solitons (DSs) in a nonlinear relativistic one-dimensional Dirac equation [14]. The DS stability, its dynamics and DSs interaction have been investigated in [19]. The formation and dynamics of two-dimensional DSs in square binary

waveguide lattices have been investigated in [20]. The higher-order Dirac solitons in BWAs have been studied in [21]. Note that nonlinear Dirac equations have been studied since a long time, e.g., by Heisenberg [22].

Quite recently, it has been shown in [23] that at the interface of two BWAs one can create the optical analog of a special state, known in the quantum field theory as a *Jackiw-Rebbi* (JR) solution [24]. The JR state led to the prediction of the charge fractionalisation phenomenon which plays a central role in the fractional quantum Hall effect [25]. One of amazing features of the JR state is the topological nature of its zero-energy solution which can be considered as a precursor to topological insulators [26]. Topological photonics has a great potential in the development of robust optical circuits [27].

In applications, WAs can be exploited for designing signal-processing circuits, in particular optical switches. It has been shown in [28] that one can change the propagation direction of the discrete soliton and reach the desirable output channel in WAs by controlling the input phase difference between excited waveguides. Other schemes of controllable and steerable soliton-based optical switching in WAs have been discussed in [29] by using the unstable soliton modes, or with the help of a linear guided wave (or defect mode) that can be generated in an inhomogeneous array. Another method to route a discrete soliton on predefined tracks in 2D WAs through interaction with a strongly confined and intense discrete soliton (also referred to as a blocker) has been proposed in [30]. As demonstrated in [30], the blockers can block and route discrete solitons in 2D networks, therefore, AND, NOT and time gating logic functions can be achieved. Two discrete solitons under normal incidence, but with an input phase difference, can also shift each other during propagation via their interaction [31]. One can steer discrete solitons in WAs by the longitudinal modulation of the nonlinearity in WAs [32]. A blocker itself can be shifted, although with more difficulties due to the Peierls - Nabarro potential in WAs, by several waveguides through interaction with a low-intensity, wide, tilted beam [33], [34]. Recently, it has been shown that one can route a discrete soliton by using a much weaker control beam in nonlinear WAs [35].

In this work we study different scenarios of the collision between JR states and DSs in a system consisting of several BWAs with alternating signs of the Dirac mass. So far, these kind of collision and interaction, to the best of our knowledge, have not been investigated. They are interesting from both fundamental and applied perspectives. We show that the collision has the resonance features for the transmitted and reflected signals, thus

Manuscript received June 26, 2017; revised October 2, 2017; accepted October 12, 2017. Date of publication October 15, 2017; date of current version November 16, 2017. This work was supported by Vietnam National Foundation for Science and Technology Development (NAFOSTED) under Grant 103.03-2016.01. (Corresponding author: Truong X. Tran).

Tr. X. Tran was with the Max Planck Institute for the Science of Light, Erlangen 91058, Germany. He is now with the Le Quy Don University, HaNoi, VietNam (e-mail: tranxr@gmail.com).

D. C. Duong was with the University of Information Technologies, Mechanics and Optics, St. Petersburg 197101, Russia. He is now with the Le Quy Don University, HaNoi, VietNam (e-mail: chi\_zung@yahoo.com).

F. Biancalana was with the Max Planck Institute for the Science of Light, Erlangen 91058, Germany. He is now with the School of Engineering and Physical Sciences, Heriot-Watt University, Edinburgh EH14 4AS, U.K. (e-mail: f.biancalana@hw.ac.uk).

Color versions of one or more of the figures in this paper are available online at <http://ieeexplore.ieee.org>.

Digital Object Identifier 10.1109/JLT.2017.2763592

the switching effect can be achieved. We show that DSs can be trapped between two JR states.

The paper is organized as follows. In Sections II and III, we investigate the collision of a DS with a JR state of the 1st and 2nd types, respectively. The interaction and trapping of DSs between two JR states are studied in Section IV. Finally, in Section V we summarize our results and finish with concluding remarks.

## II. COLLISION OF A DIRAC SOLITON WITH A JR STATE OF THE 1ST TYPE

Light propagation in a BWA with Kerr nonlinearity can be described, in the continuous-wave regime, by the following dimensionless coupled-mode equations (CMEs) [14]:

$$i \frac{da_n(z)}{dz} + \kappa [a_{n+1}(z) + a_{n-1}(z)] - (-1)^n \sigma a_n + \gamma |a_n|^2 a_n(z) = 0, \quad (1)$$

where  $a_n$  is the electric field amplitude in the  $n$ th waveguide,  $z$  is the longitudinal spatial coordinate,  $2\sigma$  and  $\kappa$  are the propagation mismatch and the coupling coefficient between two adjacent waveguides of the array, respectively, and  $\gamma$  is the nonlinear coefficient of waveguides which is positive for self-focusing, but negative for self-defocusing media. The system analyzed in this work consists of two interfaced BWAs with opposite propagation mismatches. For waveguides with  $n < 0$  we have  $\sigma = \sigma_1$ , whereas for  $n \geq 0$  we have  $\sigma = \sigma_2$ . The illustrative sketch of this system is depicted in Fig. 1(a).

After setting  $\Psi_1(n) = (-1)^n a_{2n}$  and  $\Psi_2(n) = i(-1)^n a_{2n-1}$ , and following the standard approach [12] by supposing that all beams are large enough we can introduce the continuous transverse coordinate  $\xi \leftrightarrow n$  and the two-component spinor  $\Psi(\xi, z) = (\Psi_1, \Psi_2)^T$  which satisfies the 1D nonlinear Dirac equation [14]:

$$i \partial_z \Psi = -i\kappa \hat{\sigma}_x \partial_\xi \Psi + \sigma \hat{\sigma}_z \Psi - \gamma G, \quad (2)$$

where the nonlinear terms  $G \equiv (|\Psi_1|^2 \Psi_1, |\Psi_2|^2 \Psi_2)^T$ ;  $\hat{\sigma}_x$  and  $\hat{\sigma}_z$  are the usual Pauli matrices. In quantum field theory the parameter  $\sigma$  in the Dirac equation is often called the mass of the Dirac field (or Dirac mass), and this mass parameter can be both positive and negative (see, for instance, [36] for more details).

Now we briefly re-introduce the solutions for JR states occurring at the interface between two BWAs which have been analytically found just recently [23].

If  $\sigma_1 < 0$  and  $\sigma_2 > 0$  we get the following exact localized solution of (2) in the linear case [23]:

$$\Psi(\xi) = \sqrt{\frac{|\sigma_1 \sigma_2|}{\kappa(|\sigma_1| + |\sigma_2|)}} \begin{pmatrix} 1 \\ i \end{pmatrix} e^{-|\sigma(\xi)|\xi/\kappa}. \quad (3)$$

As already mentioned in [23], the continuous solution (3) is the exact one to (2), but it is an approximate solution to the discrete (1). Obviously, this approximation will become better if the beam width gets larger so that the continuous limit  $\xi \leftrightarrow n$  is valid. For JR states, this condition can be met if  $|\sigma(\xi)|/\kappa$  is not too large. As shown in [23, Fig. 1] the continuous solution (3) is used as JR states input condition for numerically solving the discrete (1) with  $|\sigma(\xi)|/\kappa = 1$  and we have obtained a

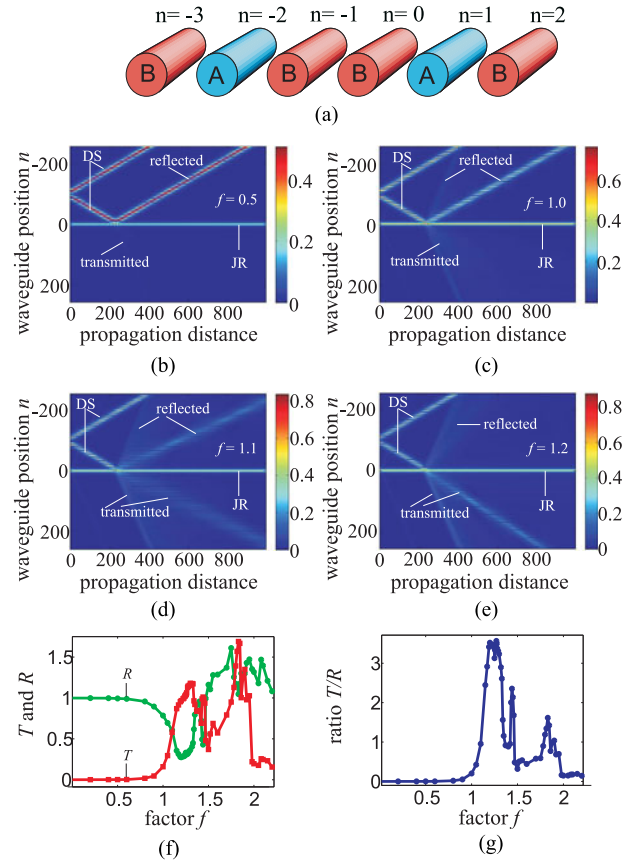


Fig. 1. (Color online) Collision between a DS and a JR state of the 1st type. (a) Illustrative sketch of two BWAs with opposite propagation mismatches located adjacent to each other. (b, c, d, e) Scenarios of collision between a DS and a JR state of the 1st type for various values of factor  $f = 0.5, 1.0, 1.1,$  and  $1.2,$  respectively. (f) The transmittance  $T$  and the reflectance  $R$  as a function of the factor  $f$ . (g) The ratio of the transmittance  $T$  to the reflectance  $R$  as a function of the factor  $f$ . Parameters:  $\sigma_1 = -0.6; \sigma_2 = 0.6; \kappa = 1; \gamma = 1;$  the width parameter for the DS  $n_0 = 5;$  total number of waveguides  $N = 1441$ .

perfectly localized beam whose shape and profile are excellently preserved during propagation in the linear regime (where the continuous solution (3) is found). This is an obvious evidence that the continuous solution (3) is an excellent approximate solution to the discrete (1) in the linear regime when  $|\sigma(\xi)|/\kappa \leq 1$ . In this work, we will use  $|\sigma| = 0.6$  and  $\kappa = 1$ , so, obviously, the condition  $|\sigma(\xi)|/\kappa \leq 1$  is held true.

If  $|\sigma_1| = |\sigma_2| = \sigma_0$  one can easily get following exact localized solutions for the discrete (1) without nonlinearity ( $\gamma = 0$ ) for the following two cases [23]:

If  $-\sigma_1 = \sigma_2 = \sigma_0 > 0$ , one gets the following JR state of the 1st type:

$$a_n = b_n e^{i[\kappa - \sqrt{\sigma_0^2 + \kappa^2}]z}, \quad (4)$$

where  $b_n$  is real and independent of the variable  $z$ ,  $b_{2n-1} = b_{2n}$ , if  $n \geq 0$  one has the following relationship:  $b_{2n}/b_{2n+1} = \alpha \equiv -[\sigma_0/\kappa + \sqrt{1 + \sigma_0^2/\kappa^2}]$ , whereas for  $n < 0$  one has:  $b_{2n+1}/b_{2n} = \alpha$ . Note that the central region for generating a JR state of the 1st type has two neighboring waveguides with  $(-1)^n \sigma$  which must be positive.

However, if  $\sigma_1 = -\sigma_2 = \sigma_0 > 0$ , one has the following JR state of the 2nd type:

$$a_n = b_n e^{i[\kappa + \sqrt{\sigma_0^2 + \kappa^2}]z}, \quad (5)$$

where  $b_n$  is again real and independent of the variable  $z$ ,  $b_{2n-1} = b_{2n}$ , if  $n \geq 0$  one has:  $b_{2n}/b_{2n+1} = -\alpha$ , whereas for  $n < 0$  one has:  $b_{2n+1}/b_{2n} = -\alpha$ . Note that the central region for generating a JR state of the 2nd type has two neighboring waveguides with  $(-1)^n \sigma$  which must be negative.

Even though the solutions in the form of (3)–(5) are obtained from the linear problem, these solutions can be successfully used to construct the initial conditions for getting the robust nonlinear localized JR states whose established profiles after a certain propagation distance are just slightly different from the input conditions [23].

Regarding the Dirac soliton solution in BWAs, we have obtained it in the form of [14, eq. (6)]. Because this Dirac soliton solution has been well investigated in [14], [19]–[21], therefore, we will not include it here. Although this Dirac soliton solution is also derived in the continuous limit when  $\xi \leftrightarrow n$ , nonetheless, as demonstrated in [14], it is an excellent approximate solution to the nonlinear discrete (1) when the width parameter  $n_0$  of the Dirac soliton is large enough so that  $n_0|\sigma| > \kappa$ . In this work, we will use  $|\sigma| = 0.6$ ,  $\kappa = 1$ , and  $n_0 = 5$ , so, obviously, the condition  $n_0|\sigma| > \kappa$  is also held true.

Now it is time for us to proceed further with numerical simulations. It is worth emphasizing that all numerical simulations in this work are performed by directly solving the discrete (1). At the beginning, we investigate the collision of a Dirac soliton with a JR state of the 1st type. In order to do that one needs to create a DS which propagates obliquely. This is easily done by launching two initially out-of-phase DSs which are transversely motionless at the very beginning [19] as shown in Fig. 1(b)–(e). Due to the interaction between these two out-of-phase DSs after some short propagation distance one will get two DSs which propagate obliquely in opposite directions. The downward propagating DS will collide with a JR state of the 1st type located at the central region of the waveguide array. In Fig. 1 we fix the parameters for the DS, but change the JR state in the form of (3) by multiplying it by a factor  $f$ . Note that in the nonlinear case, this initial condition is not the exact solution for the nonlinear JR state, however, as pointed out in [23], if  $f$  is small enough, after some propagation distance the nonlinear JR state will be established with profile just slightly different from the input one. The parameters for generating the DSs and JR state in Fig. 1 are as follows: the initial distance between two DSs is 20 waveguides; the Dirac mass for the upper BWA ( $n < 0$ ) is  $\sigma_1 = -0.6$ ; whereas for the lower BWA  $\sigma_2 = 0.6$ ; the coupling coefficient between two adjacent waveguides  $\kappa = 1$ ; the nonlinear coefficient  $\gamma = 1$  for all waveguides; the width parameter for DSs  $n_0 = 5$  (for DS solutions, see [14, eq. (6)] for more details); and the total number of waveguides  $N = 1441$ . In Fig. 1(b) with  $f = 0.5$ , after the collision another localized DS is formed as the reflected beam, and only very weak transmitted signal is hardly observed. When  $f = 1$  as shown in Fig. 1(c) the transmitted signal becomes stronger as compared

to Fig. 1(b). The reflected signal in Fig. 1(c) consists of two parts: one is a localized strong DS, another is a weak scattered beam which broadens quickly during propagation. If the factor  $f$  is increased further to a value of 1.1 as in Fig. 1(d) the transmitted signal becomes even stronger and one can observe that a localized DS is formed in the transmitted signal together with a weak scattered beam. Meanwhile, the reflected signal becomes weaker as compared to Fig. 1(c) and also consists of a localized DS together with a weak scattered beam. In Fig. 1(e) when  $f = 1.2$  the reflected signal is very weak and just consists of a weak scattered beam (without any DS). On the contrary, the transmitted signal is very strong in Fig. 1(e) and consists of a strong localized DS together with a scattered beam.

Now we analyze the power of the reflected and transmitted beams at the propagation distance  $z = 600$ . At this distance one can sum up all  $|a_n|^2$  with  $n < -40$  and get the power for the reflected beam, then take the ratio of this reflected power to the power of the incident DS to get the reflectance  $R$ . Analogously, one can get the transmittance  $T$  for all waveguides with  $n > 40$ . The central region of the waveguide array with  $-40 < n < 40$  is the region for the JR state which is well separated from the reflected and transmitted beams at the propagation distance  $z = 600$ . In Fig. 1(f) we plot the transmittance  $T$  and the reflectance  $R$ , and in Fig. 1(g) we plot the ratio of the transmittance  $T$  to the reflectance  $R$  as a function of the factor  $f$ . As seen from Fig. 1(f) and (g) when  $f < 0.7$  the reflectance is high ( $R \simeq 1$ ) and the transmittance is very low ( $T \simeq 0$ ) (see also Fig. 1(b)). However, when  $f$  is increased further up to unity the reflectance  $R$  gradually decreases, whereas the transmittance  $T$  gradually increases (see also Fig. 1(c)). In particular, when  $f$  is increased from 1.0 to 1.2 we get the resonance when  $R$  sharply decreases and  $T$  sharply increases. This feature is also clearly illustrated in Fig. 1(e) where only a very weak scattered beam is observed for the reflected signal, but very strong beam is generated for the transmitted signal. It is peculiar to see in Fig. 1(f) that the reflectance  $R$  and transmittance  $T$  can be larger than unity. This is due to the fact that both reflected and transmitted signals can take the energy of the JR state. In Fig. 1(f) and (g) one can see several resonance peaks around  $f = 1.2, 1.44$ , and  $1.83$ . If we continue to increase  $f$ , we will get other resonance peaks. However, when  $f$  is too large ( $f > 2$ ), the *linear* (with  $\gamma = 0$ ) localized solution of the JR state in the form of (3) multiplied by the factor  $f$  will be a bad approximation for the *nonlinear* (1) (with  $\gamma \neq 0$ ). That is the reason why we just focus on small values of  $f$  in Fig. 1.

### III. COLLISION OF A DIRAC SOLITON WITH A JR STATE OF THE 2ND TYPE

Now we investigate the collision of a Dirac soliton with JR states of the 2nd type. All parameters of the waveguide array used in this Section are the same as in Section II with the exception that now we change the sign of both  $\sigma_1$  and  $\sigma_2$ . This is necessary to create right conditions for generating JR states of the 2nd type: the central region for generating a JR state of the 2nd type has two neighboring waveguides with  $(-1)^n \sigma$  which must be negative. Like in Section II, the central region

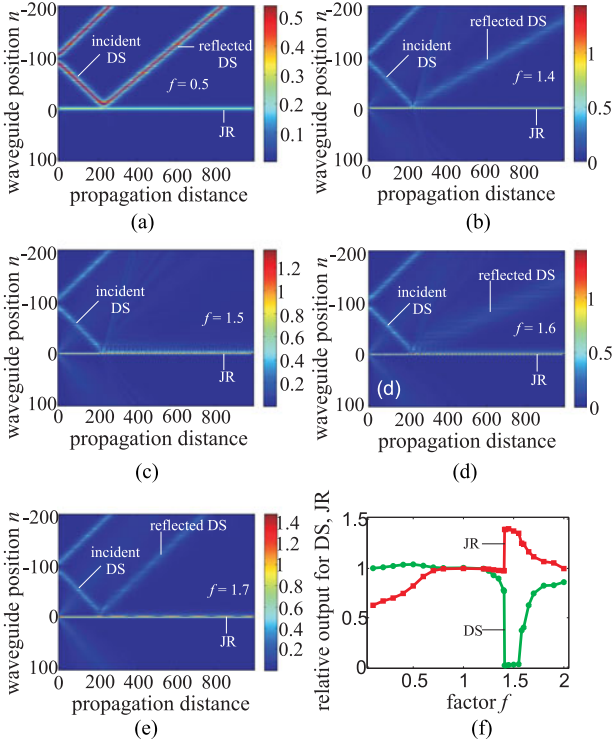


Fig. 2. (Color online) Collision between a DS and a JR state of the 2nd type. (a, b, c, d, e) Scenarios of collision between a DS and a JR state of the 2nd type for various values of factor  $f = 0.5, 1.4, 1.5, 1.6,$  and  $1.7$ , respectively. (f) The green curve represents the relative power ratio of the reflected DS to the incident DS as a function of the factor  $f$ , whereas the red curve represents the relative power ratio of the output JR state to the input JR state. Parameters:  $\sigma_1 = 0.6; \sigma_2 = -0.6; \kappa = 1; \gamma = 1$ ; the width parameter for the DS  $n_0 = 5$ .

of the JR state in this Section is two waveguides with  $n = -1$  and  $0$ . Now we need to use the linear localized solution in the form of (5) to construct the initial condition for the nonlinear JR state of the 2nd type. The initial amplitude of the JR state of the 2nd type at the central region is as follows:  $a_{-1} = a_0 = f\sqrt{|\sigma_1\sigma_2|/(\kappa(|\sigma_1| + |\sigma_2|))}$  with  $f$  being varied. Once the peak amplitude of the JR state is fixed, one can easily construct all of its profile as indicated in Section II. In Fig. 2(a)–(e) we investigate different scenarios of the collision of a Dirac soliton with JR states of the 2nd type for different values of  $f = 0.5, 1.4, 1.5, 1.6,$  and  $1.7$ . Unlike cases shown in Fig. 1, one can easily see from Fig. 2(a)–(e) that the transmitted signal is very weak. Regarding the reflected signal in Fig. 2(a) when  $f = 0.5$  one obtains only a very strong reflected DS, whereas in Fig. 2(b) when  $f = 1.4$  one gets some weak scattered beam and a reflected DS which is weaker than the reflected DS in Fig. 2(a). Another big difference between Figs. 1 and 2 is that the slope of the reflected DS in Fig. 1 remains almost the same, whereas it changes in Fig. 2. First, when  $f$  is small the slope of the reflected DS decreases if  $f$  gets increased as shown in Fig. 2(a) and (b). If we increase  $f$  further as in Fig. 2(c) the slope of the reflected DS decreases to a degree that the reflected DS becomes parallel to the JR state, as a result, the reflected DS is merged into the JR state. If we continue to increase the value of  $f$  as shown in Fig. 2(d) and (e) the slope of the reflected DS will increase, as a result, the reflected DS will be separated

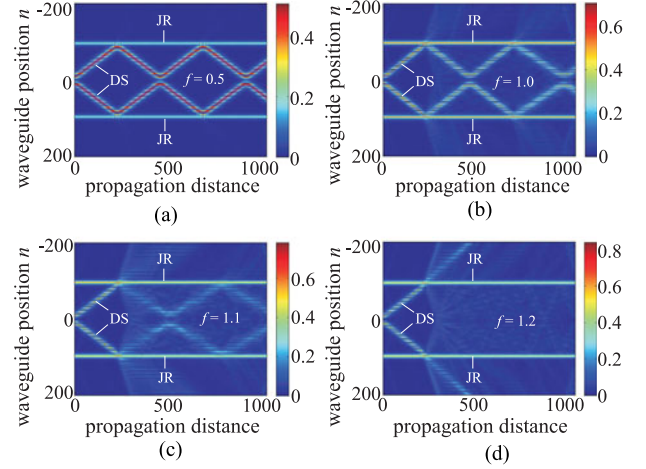


Fig. 3. (Color online) (a, b, c, d) Interaction of two Dirac solitons with two JR states of the 1st type for various values of the factor  $f = 0.5, 1.0, 1.1,$  and  $1.2$ . The distance between two JR states is equal to 200 waveguides. The first BWA has waveguide positions  $n \leq -100$  with the Dirac mass  $\sigma_1 = 0.6$ ; the second BWA has waveguide positions  $-99 \leq n \leq 99$  with the Dirac mass  $\sigma_2 = -0.6$ ; whereas the third BWA has waveguide positions  $n \geq 100$  with the Dirac mass  $\sigma_3 = 0.6$ . Other parameters are the same as in Fig. 1.

from the JR state, and one can observe the reflected DS again. The green curve in Fig. 2(f) represents the relative output power of the reflected DS (taken at the propagation distance  $z = 900$ ) to the input power of the incident DS (taken at  $z = 0$ ). The red curve in Fig. 2(f) represents the relative output power of the JR state, i.e., the ratio of the output power of the JR state (taken at the propagation distance  $z = 900$ ) to the input power of the JR state taken at the propagation distance  $z = 140$ . Note that we do not take the input power of the JR state at  $z = 0$ , because as seen in Fig. 2(b)–(e) (when  $f$  is large) at the very beginning of propagation some portion of the JR state energy is radiated away, and the stable profile of the JR state is established at the propagation distance  $z \simeq 100$  before the collision at the distance  $z \simeq 200$ . As seen in Fig. 2(f) one gets a very sharp resonance around  $f = 1.5$ .

#### IV. INTERACTION OF DIRAC SOLITONS WITH TWO JR STATES

The features occurring during collision of a DS with a JR state analyzed in Sections II and III can be used to manipulate DSs such as switching or steering. In this Section we investigate the possibility of trapping the DSs inside two “walls” created by two JR states. In this case, the systems shown in Figs. 3 and 4 consist of three binary waveguide arrays with two interfaces for generating JR states. These two interfaces are located at waveguides with position  $n = (-100, -99)$  and  $(99, 100)$ , thus, the distance between two JR states is 200 waveguides. The first BWA has waveguide positions  $n \leq -100$  with the Dirac mass  $\sigma_1$ ; the second BWA has waveguide positions  $-99 \leq n \leq 99$  with the Dirac mass  $\sigma_2$ ; whereas the third BWA has waveguide positions  $n \geq 100$  with the Dirac mass  $\sigma_3$ .

In Fig. 3(a)–(d) two JR states of the 1st type are used to construct the trap with various values of  $f = 0.5, 1.0, 1.1,$  and  $1.2$ , respectively. In order to be able to generate JR states of the

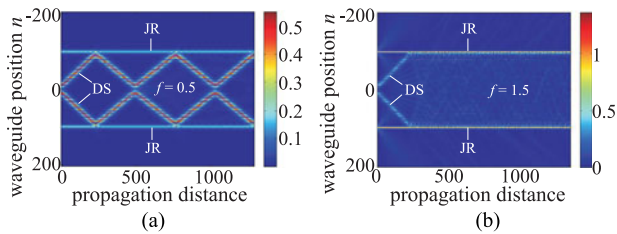


Fig. 4. (Color online) (a, b) Interaction of two Dirac solitons with two JR states of the 2nd type for two values of the factor  $f = 0.5$  and  $1.5$ . The distance between two JR states is equal to 200 waveguides. The first BWA has waveguide positions  $n \leq -100$  with the Dirac mass  $\sigma_1 = -0.6$ ; the second BWA has waveguide positions  $-99 \leq n \leq 99$  with the Dirac mass  $\sigma_2 = 0.6$ ; whereas the third BWA has waveguide positions  $n \geq 100$  with the Dirac mass  $\sigma_3 = -0.6$ . Other parameters are the same as in Fig. 2.

1st type in Fig. 3 we chose  $\sigma_1 = -\sigma_2 = \sigma_3 = 0.6$ . In Fig. 3(a) (when the factor  $f = 0.5$ ) the two DSs are well trapped between two JR states. After each collision DSs are well reflected backwards to the region between two JR states. This result is in agreement with the scenario shown in Fig. 1(b). When  $f$  is increased to 1.0 and 1.1 as shown in Fig. 3(b) and (c) the transmitted signal becomes more and more pronounced, as a result, some portion of the DSs energy escapes from the trap (see also Fig. 1(c) and (d)). In particular, in Fig. 3(d) when  $f = 1.2$  we again observe the resonance in which almost all energy of two DSs escapes the trap, and as a result, only a negligible portion of DSs energy gets trapped inside the walls created by two JR states. This behavior shown in Fig. 3(d) is in agreement with the scenarios shown in Fig. 1(e)–(g). Thus, one can use two JR states of the 1st type to manipulate the trapping and escaping effects of Dirac solitons.

In Fig. 4(a) and (b) two JR states of the 2nd type are used to construct the trap with factor  $f = 0.5$ , and  $1.5$ , respectively. In order to be able to generate JR states of the 2nd type in Fig. 4 we chose  $\sigma_1 = -\sigma_2 = \sigma_3 = -0.6$ . In Fig. 4(a) (when the factor  $f = 0.5$ ) the two DSs are well trapped between two JR states. After each collision DSs are well reflected backwards to the region between two JR states (see also Fig. 2(a)). When  $f$  is increased to 1.5, as shown in Fig. 4(b), the structure of DSs is quickly destroyed after collision, i.e., most of energy of DSs is combined together with JR states by distributing it to the waveguides close to inner sides of the walls (see also Fig. 2(c)). Thus, one also can use two JR states of the 2nd type to manipulate the trapping effects of Dirac solitons.

For estimation we use typical parameters in BWAs in [12] where the coupling coefficient in physical units  $\kappa = 140 \text{ m}^{-1}$ . Because the propagation mismatch  $\sigma$  can be easily experimentally varied in the range from  $0.5\kappa$  to  $2.1\kappa$  in [12], so in our work we can use the propagation mismatch in physical units  $\sigma = 0.6\kappa = 84 \text{ m}^{-1}$ . The typical nonlinear coefficient in physical units  $\gamma = 6.5 \text{ m}^{-1} \text{ W}^{-1}$  can be taken from [37]. In this case, the power scale will be  $P_0 = \kappa/\gamma = 21.5 \text{ W}$  and the length scale in the propagation direction will be  $z_0 = 1/\kappa = 7.1 \text{ mm}$ . As mentioned above, the total number of waveguides  $N = 1441$  is used in simulations, but this number can be much decreased, for instance, by putting two Dirac solitons much closer to the JR states at the input.

## V. SUMMARY

In conclusion, we demonstrate numerically that the collision between Dirac solitons and Jackiw-Rebbi states of the 1st type in a system consisting of several binary waveguide arrays with alternating signs of the Dirac mass can generate reflected and transmitted Dirac solitons. When the input power of the JR state of the 1st type is weak most of the energy of the Dirac soliton is reflected, whereas for certain ranges of the input power of the JR state most of the energy of the Dirac soliton is transmitted through the JR state. However, if a Dirac soliton collide with a JR state of the 2nd type, then only reflected Dirac solitons can be generated, and almost nothing is transmitted through the JR state. For certain ranges of the input power of the JR state of the 2nd type the reflected Dirac soliton propagates parallel to the JR state, such that the separated reflected Dirac soliton does not exist in this case. All of these features have resonance characters and can be used to manipulate Dirac solitons, such as steering or trapping them inside two JR states. Our results suggest that a system consisting of several BWAs with alternating signs of the Dirac mass can be used as a classical simulator to investigate the interaction between relativistic Dirac solitons and Jackiw-Rebbi states. This kind of interaction can be useful for optical switching and trapping effects.

## REFERENCES

- [1] D. N. Christodoulides, F. Lederer, and Y. Silberberg, "Discretizing light behaviour in linear and nonlinear waveguide lattices," *Nature*, vol. 424, pp. 817–823, Aug. 2003.
- [2] A. L. Jones, "Coupling of optical fibers and scattering in fibers," *J. Opt. Soc. Amer.*, vol. 55, pp. 261–271, Mar. 1965.
- [3] D. N. Christodoulides and R. I. Joseph, "Discrete self-focusing in nonlinear arrays of coupled waveguides," *Opt. Lett.*, vol. 13, pp. 794–796, Sep. 1988.
- [4] Y. S. Kivshar and G. P. Agrawal, *Optical Solitons: From Fiber to Photonic Crystals*, 5th ed. New York, NY, USA: Academic, 2003.
- [5] G. P. Agrawal, *Applications of Nonlinear Fiber Optics*, 2nd ed. New York, NY, USA: Academic, 2008.
- [6] T. X. Tran and F. Biancalana, "Diffractive resonant radiation emitted by spatial solitons in waveguide arrays," *Phys. Rev. Lett.*, vol. 110, pp. 113903–113906, Mar. 2013.
- [7] T. X. Tran and F. Biancalana, "Mimicking the nonlinear dynamics of optical fibers with waveguide arrays: Towards a spatiotemporal supercontinuum generation," *Opt. Express*, vol. 21, pp. 17539–17546, Jul. 2013.
- [8] T. X. Tran, D. C. Duong, and F. Biancalana, "Supercontinuum generation in both frequency and wave number domains in nonlinear waveguide arrays," *Phys. Rev. A*, vol. 89, pp. 013826–013831, Jan. 2014.
- [9] T. Pertsch, P. Dannberg, W. Elfein, A. Bräuer, and F. Lederer, "Optical Bloch oscillations in temperature tuned waveguide arrays," *Phys. Rev. Lett.*, vol. 83, pp. 4752–4755, Dec. 1999.
- [10] G. Lenz, I. Talanina, and C. M. de Sterke, "Bloch oscillations in an array of curved optical waveguides," *Phys. Rev. Lett.*, vol. 83, pp. 963–966, Aug. 1999.
- [11] M. Ghulinyan, C. J. Oton, Z. Gaburro, L. Pavesi, C. Toninelli, and D. S. Wiersma, "Zener tunneling of light waves in an optical superlattice," *Phys. Rev. Lett.*, vol. 94, pp. 127401–127404, Apr. 2005.
- [12] F. Dreisow *et al.*, "Classical simulation of relativistic Zitterbewegung in photonic lattices," *Phys. Rev. Lett.*, vol. 105, pp. 143902–143905, Oct. 2010.
- [13] F. Dreisow, R. Keil, A. Tünnermann, S. Nolte, S. Longhi, and A. Szameit, "Klein tunneling of light in waveguide superlattices," *Europhys. Lett.*, vol. 97, pp. 10008–10013, Jan. 2012.
- [14] T. X. Tran, S. Longhi, and F. Biancalana, "Optical analogue of relativistic Dirac solitons in binary waveguide arrays," *Ann. Phys.*, vol. 340, pp. 179–187, Jan. 2014.
- [15] A. A. Sukhorukov and Y. S. Kivshar, "Generation and stability of discrete gap solitons," *Opt. Lett.*, vol. 28, pp. 2345–2347, Dec. 2003.

- [16] M. Conforti, C. De Angelis, and T. R. Akylas, “Energy localization and transport in binary waveguide arrays,” *Phys. Rev. A*, vol. 83, pp. 043822–043827, Apr. 2011.
- [17] R. Morandotti *et al.*, “Observation of discrete gap solitons in binary waveguide arrays,” *Opt. Lett.*, vol. 29, pp. 2890–2892, Dec. 2004.
- [18] M. Johansson, K. Kirr, A. S. Kovalev, and L. Kroon, “Gap and out-gap solitons in modulated systems of finite length: Exact solutions in the slowly varying envelope limit,” *Physica Scripta*, vol. 83, pp. 065005–065016 May 2011.
- [19] T. X. Tran, X. N. Nguyen, and D. C. Duong, “Dirac soliton stability and interaction in binary waveguide arrays,” *J. Opt. Soc. Amer. B*, vol. 31, pp. 1132–1136, Apr. 2014.
- [20] T. X. Tran, X. N. Nguyen, and F. Biancalana, “Dirac solitons in square binary wave guide lattices,” *Phys. Rev. A*, vol. 91, pp. 023814–023820, Feb. 2015.
- [21] T. X. Tran and D. C. Duong, “Higher-order Dirac solitons in binary waveguide arrays,” *Ann. Phys.*, vol. 361, pp. 501–508, Jul. 2015.
- [22] W. Heisenberg, “Quantum theory of fields and elementary particles,” *Rev. Modern Phys.*, vol. 29, pp. 269–278, 1957.
- [23] T. X. Tran and F. Biancalana, “Linear and nonlinear photonic Jackiw-Rebbi states in interfaced binary waveguide arrays,” *Phys. Rev. A*, vol. 96, pp. 013831–013835, Jul. 2017.
- [24] R. Jackiw and C. Rebbi, “Solitons with fermion number  $1/2$ ,” *Phys. Rev. D*, vol. 13, pp. 3398–3409, Jun. 1976.
- [25] R. B. Laughlin, “Nobel Lecture: Fractional quantization,” *Rev. Mod. Phys.*, vol. 71, pp. 863–874, Jul. 1999.
- [26] M. Z. Hasan and C. L. Kane, “*Colloquium*: Topological insulators,” *Rev. Mod. Phys.*, vol. 82, pp. 3045–3067, Nov. 2010.
- [27] M. C. Rechtsman *et al.*, “Photonic Floquet topological insulators,” *Nature (London)*, vol. 496, pp. 196–200, Apr. 2013.
- [28] W. Królikowski, U. Trutschel, M. Cronin-Golomb, and C. Schmidt-Hattenberger, “Solitonlike optical switching in a circular fiber array,” *Opt. Lett.*, vol. 19, pp. 320–322, Mar. 1994.
- [29] W. Królikowski and Y. S. Kivshar, “Soliton-based optical switching in waveguide arrays,” *J. Opt. Soc. Amer. B*, vol. 13, pp. 876–887, May 1996.
- [30] D. N. Christodoulides and E. D. Eugenieva, “Blocking and routing discrete solitons in two-dimensional networks of nonlinear waveguide arrays,” *Phys. Rev. Lett.*, vol. 87, pp. 233901–233904, Nov. 2001.
- [31] J. Meier, G. I. Stegeman, Y. Silberberg, R. Morandotti, and J. S. Aitchison, “Nonlinear optical beam interactions in waveguide arrays,” *Phys. Rev. Lett.*, vol. 93, pp. 093903–093906, Aug. 2004.
- [32] G. Assanto, L. A. Cisneros, A. A. Minzoni, B. D. Skuse, N. F. Smyth, and A. L. Worthy, “Soliton steering by longitudinal modulation of the nonlinearity in waveguide arrays,” *Phys. Rev. Lett.*, vol. 104, pp. 053903–053906, Feb. 2010.
- [33] O. Bang and P. D. Miller, “Exploiting discreteness for switching in waveguide arrays,” *Opt. Lett.*, vol. 21, pp. 1105–1107, Aug. 1996.
- [34] J. Meier *et al.*, “Beam interactions with a blocker soliton in one-dimensional arrays,” *Opt. Lett.*, vol. 30, pp. 1027–1029, May 2005.
- [35] T. X. Tran and Q. Nguyen-The, “Controlling a discrete soliton by a weak beam in waveguide arrays,” *J. Lightw. Technol.*, vol. 34, no. 17, pp. 4104–4109, Sep. 2016.
- [36] R. Keil *et al.*, “Optical simulation of charge conservation violation and Majorana dynamics,” *Optica*, vol. 2, pp. 454–459, May 2015.
- [37] R. Morandotti, U. Peschel, J. S. Aitchison, H. S. Eisenberg, and Y. Silberberg, “Experimental observation of linear and nonlinear optical Bloch oscillations,” *Phys. Rev. Lett.*, vol. 83, pp. 4756–4759, Dec. 1999.

**Truong X. Tran** received the B.S. and M.S. degrees in laser techniques and laser technologies from the St. Petersburg National Research University of Information Technologies, Mechanics and Optics, St. Petersburg, Russia, in 2002 and 2004, respectively, and the Ph.D. degree in optics from the same university in 2007. In 2009–2012, he was a Postdoctoral Researcher at the Max Planck Institute for the Science of Light, Erlangen, Germany. Since 2013, he has been a Lecturer at the Department of Physics, Le Quy Don University, HaNoi, VietNam. He is the author of about 35 scientific articles in peer-reviewed journals. His research interests include fiber optics, optical solitons, waveguide arrays, photonic crystal fibers, simulation of quantum effects with optical platforms, and laser technologies. He won a project to establish a German Max Planck Partner Group in HaNoi from 2013 to 2016.

**Dũng C. Duong** received the B.S. and M.S. degrees in laser techniques and laser technologies from St. Petersburg National Research University of Information Technologies, Mechanics and Optics, St. Petersburg, Russia, in 2002 and 2004, respectively, and the Ph.D. degree in optics from the same university in 2007. Since 2007, he has been a Lecturer at the Department of Physics, Le Quy Don University, HaNoi, VietNam. He is the author of about 15 scientific articles in peer-reviewed journals. His research interests include fiber optics, electro-optics, and laser technologies.

**Fabio Biancalana** received the “Laurea” degree in theoretical particle physics from the University of Roma III, Rome, Italy, in 2001. He received the Ph.D. project at the University of Bath, U.K. He received an IRCSET Postdoctoral Fellowship (2006) at the Tyndall National Institute in Cork (Ireland). In 2007, he moved to Cardiff University, U.K., where he holds an EPSRC Fellowship in theoretical physics. In 2009–2014, he was the Leader of the Max Planck Research Group on “Nonlinear Photonic Nanostructures” at the Max Planck Institute for the Science of Light in Erlangen, Germany. He joined Heriot-Watt as a Reader in 2012. He is the author of about 80 papers in peer-reviewed journals. His research interests include fiber optics, optical solitons, waveguide arrays, photonic crystal fibers, simulation of quantum effects with optical platforms, plasmonics, and graphenes.